Leukocyte depletion in dried blood spot cards enables enrichment of parasite DNA for improved sequencing

Allison J. Tierney[1], Surendra K. Prajapati[2,3], Alec Leonetti[4], Abebe A. Fola[4], Sebastian Shine Kwapong[5], Keith R. Baillargeon,[1] Ashleigh Roberds[6,7], V. Ann Stewart[6], Linda E. Amoah[5], Jeffrey A. Bailey[4], Kim C. Williamson[2], and Charles R. Mace[1]*

[1] Department of Chemistry, Tufts University, Medford, MA, USA

[2] Department of Microbiology and Immunology, Uniformed Services University of the Health Sciences, Bethesda, MD, USA

[3] Henry M. Jackson Foundation for the Advancement of Military Medicine, Inc., Rockville, MD, USA

[4] Department of Pathology and Laboratory Medicine, Warren Alpert Medical School, Brown University, Providence, RI, USA

[5] Immunology Department, Noguchi Memorial Institute of Medical Research, University of Ghana, Accra, Ghana

[6] Department of Preventive Medicine and Biostatistics, Uniformed Services University of the Health Sciences, Bethesda, MD, USA

[7] Bacterial Diseases Branch, Center for Infectious Disease Research, Walter Reed Army Institute of Research, Silver Spring, MD, USA

* Corresponding author email: charles.mace@tufts.edu

Keywords: dried blood spots, microsampling, leukocyte depletion, malaria, sequencing

Abstract

Expanding access to simple blood collection tools is essential to monitor, control, and eliminate malaria in low resource settings where the disease is endemic. The most common method to preserve blood is depositing fingerstick samples onto filter paper—the dried blood spot (DBS) card. While DBS cards offer more optimal storage solutions than venous blood in vacutainers, they do not provide sample cleanup or enrichment of *Plasmodium* DNA. These samples retain high host-to-parasite DNA ratios, which negatively affect the quality of downstream sequencing. We developed a Leukocyte Depletion Card (LDC) that substantially depletes host white blood cells from whole blood to enrich *Plasmodium*-infected red blood cells in a hematocrit-independent volume (9.0 ± 0.5 µL). Using quantitative PCR, we evaluate the performance of the LDC using blood collected from 16 *P. falciparum*-infected patients at a clinic in Cape Coast, Ghana. The LDC achieved an average 32.5-fold parasite enrichment over venous blood. Promisingly, the LDC also provides a 36.6-fold parasite enrichment over a DBS card. Initial testing of targeted sequencing demonstrates significant ($p < 0.01$) improvement in *P. falciparum* read counts and coverage for the LDC. The LDC represents a unique microsampling device with potential applications in epidemiological studies of malaria.

1 Introduction

Malaria remains a major public health challenge, particularly in sub-Saharan Africa, where *Plasmodium falciparum* is the most prevalent and deadly species of parasite[1]. Sampling blood from malaria-infected patients is crucial to molecular and epidemiological studies that aid in understanding, managing, and controlling malaria. Currently, the primary method for blood collection and storage for molecular analysis is the dried blood spot (DBS) card (e.g., Whatman 903 Protein Saver cards). Despite the convenience and ease of sampling and storage, 903 cards are limited by their simple design, leading to a range of possible user errors (e.g., unreliable zone filling) and inconsistent sample extraction.[2–5] Moreover, DNA extracted from 903 cards is often significantly contaminated with host DNA, which dilutes the targeted parasite DNA.[6] Even in samples with moderate levels of parasitemia (e.g., 1%), where the parasites are more abundant than host white blood cell (WBC) DNA, the larger size of the diploid human genome (6.4 GB) overshadows the smaller, haploid genome of the parasite (22.8 MB)—a 280-fold difference in size.[7] While challenges related to analyzing these relatively small amounts of parasite genetic material have been extensively addressed by modifying current sequencing methods (e.g., amplification additives[8]) or improving sample enrichment methods (e.g., hybrid capture using whole genome baits[6], or synthetic oligonucleotide probes[9]), contamination from the host remains an outstanding obstacle. This issue is particularly pronounced in technologies available to those in limited resource settings. Additionally, the presence of host genes and proteins severely affects the efficiency of downstream analyses, leading to off-target sequencing and reduced sequence coverage of the target *Plasmodium* genome.[10]

Methods to remove host cell contamination in field-collected samples of blood include a range of chemical and physical processes. Enzymatic treatments (e.g., methylation dependent enzyme digestion)[6] can enrich *Plasmodium* DNA up to 9-fold by selectively degrading host DNA. Common density gradient media (e.g., Ficoll, Lymphoprep) have been shown to offer between 40–80% WBC depletion,[11,12] while Pall Acrodisc WBC syringe filters and Plasmodipur filters have

been shown to provide 40–100%[13] and 12–54%[10] depletion, respectively. In addition to single isolation methods, combination methods of density gradient media and filter units (e.g., Lymphoprep + Plasmodipur + antiHLA1)[10] have been shown to deplete 75–98% of WBCs. Unfortunately, approaches relying on filtration require relatively large volumes of venous blood (1–10 mL, at minimum) and active processing at the point of sampling by a healthcare worker using intensive protocols. Leukosorb, a fibrous membrane used in commercially-available filter units to recover WBCs selectively,[14,15] is translatable to the development of paper-based devices and can accommodate fingerstick volumes of blood (40–70 μL cm^{-1}).[16] We have previously used Leukosorb as a pre-filter for plasma separation devices that can recover liquid[17] or dried[18] plasma from whole blood. We hypothesized that using Leukosorb as the basis of a simple, field-deployable card (a Leukocyte Depletion Card; LDC) would cause the spatial separation of host WBCs from parasite-infected red blood cells (RBCs) and result in improved recovery and analysis of *Plasmodium* DNA.

We first tested the LDC using *in vitro*, contrived samples of parasitized blood to demonstrate how card design elements (i) enriched the recovery of parasite DNA over host DNA compared to the 903 card, while (ii) maintaining quantitative recovery of parasite DNA from infected RBCs. Following this characterization, we assessed the clinical performance of the LDC with whole blood samples from 16 patients, which varied in WBC and parasite counts. In comparison to the 903 card, the LDC showed superior WBC depletion and fold parasite enrichment, resulting in significant improvements to *Plasmodium* sequencing results (both read count and read coverage) for patients with parasitemias above 4046 parasites μL^{-1}. By intrinsically depleting WBCs and retaining parasitized RBCs—without requiring any additional steps by a patient or healthcare worker collecting blood in a field setting—the LDC has the potential to advance genomic, epidemiological studies of malaria, such as improving the accuracy and scope of malaria drug- and drug-resistant[19,20] tracking and public health monitoring.

2 Results and Discussion

2.1 Designing and testing consistent filling of card prototypes across a range of hematocrits

Cards must optimally (i) fill across a wide hematocrit range to accommodate the variable composition of blood anticipated in a broad patient population, (ii) dry in less than 3 hours to promote biomolecule stability (i.e., DNA, RNA, proteins), (iii) provide a hematocrit-independent, single extraction punch volume to allow for quantitative leukocyte and parasite counts, and (iv) be operationally simple in the environments where they are intended to be handled (i.e., field settings and clinical laboratories).[21] Based on these design criteria, we used our previously reported observations of blood cell transport in paper-based devices to design candidate prototypes.[22–24] Each candidate comprised an (i) inlet zone, (ii) separation channel, (iii) extraction zone, and (iv) overflow channel as shown in **Figure 1A**. The overflow channel, which extends beyond the extraction zone, ensures complete filling of extraction zones regardless of the hematocrit of the applied sample of blood.[25,26] Further, designing devices that provide a patient-independent and reproducible volume stored in the extraction zone enables more quantitative analyses and inference of absolute input amounts (e.g., parasitemia per microliter of peripheral blood).[26] As a result of these design criteria, we evaluated four prototypes of a DBS card that could deplete WBCs: *prototype 1* (**Figure S1A,B**), *prototype 2* (**Figure S2A,B**), *prototype 3* (**Figure S3A,B**), and *prototype 4* (**Figure 1A,B**). These prototypes differed in material choice (e.g., TFN cardstock or Leukosorb) or assembly (e.g., channels with or without separate sample addition layers) to promote RBC transport to the extraction punch zone while restricting WBC movement.

We challenged each prototype with 50 µL of whole blood via pipette with contrived hematocrits ranging from 25–55%. We ensured that the entirety of the extraction zone filled for all four prototypes (**Figures 1C**, **S1C, S2C, S3C**). After drying the cards overnight, we determined the volume of blood contained in each extraction zone by quantifying the amount of hemoglobin contained in the punch. Based on the results of our earlier studies with designing DBS cards that meter whole blood, we expected that if the hematocrit did not have a significant effect on the

volume of blood recovered in a punch, we could use a single volume as a liquid reference for any patient to compare to the extracted punch.[26] *Prototypes 1*, *2*, and *3* provided punch volumes of 13.0, 18.4, and 9.7 µL, respectively (**Figures S1D, S2D, S3D**), when averaged across the entire range of hematocrits (**Table S1**); however, these numbers varied significantly between hematocrits (ANOVA, $p < 0.001$ for all three prototypes). Alternatively, *prototype 4* provided an average punch volume of 9.0 µL that did not vary significantly between hematocrits ($p = 0.11$, **Figure 1D**). Although *prototype 3* did not provide hematocrit independence across the entire range tested, volumes were statistically indifferentiable across a narrower range of hematocrits (25–50%; $p = 0.06$). As it is anticipated that patients infected with malaria are unlikely to have high hematocrits,[27,28] we chose to move forward with both *prototype 3* and *prototype 4* to test the ability of each card to deplete WBCs.

2.2 WBC depletion using healthy donor blood

To determine WBC depletion provided by *prototypes 3* and *4*, we quantified the amount of *β-actin,* a common human reference gene, present in the sample via quantitative PCR using a single donor (WBC count of 6300 μL^{-1}). To ensure analyses were comparable across different card types, we compared raw Ct values measured from a punch from each card to a matched liquid reference volume: 50 µL (903 card as a microsampling comparator), 9.7 µL (prototype 3), and 9.0 µL (*prototype 4*) (**Table S2**). *Prototype 4* depleted significantly more WBCs (higher Ct value) than the 903 card (ANOVA, $p < 0.001$) or *prototype 3* (ANOVA, $p = 0.009$). Based on these results, we chose to move forward with *prototype 4* as our final Leukocyte Depletion Card (LDC) to be tested against both contrived samples of whole blood containing RBCs infected with *in vitro* cultures of *P. falciparum* and also clinical samples of whole blood collected at a field site.

2.3 Analyzing parasite recovery using Plasmodium falciparum-infected samples from in vitro cultures

We generated contrived samples of *Plasmodium falciparum*-infected blood by supplementing whole blood from a single donor with cultures of synchronized, ring-stage parasites (NF54) at parasitemias of 0.001%, 0.01%, 0.1%, 1%, and 5% infected RBCs. Because we used a single donor to prepare samples, the total WBC count and hematocrit (40%) did not vary across parasitemias. We applied 50 µL of each sample of blood to replicate zones of a 903 card and an LDC (N = 5 zones per parasitemia). We quantified WBC and parasite DNA (*β-actin* and *spb1* genes, respectively) from punches and matched volumes of a liquid reference sample (50 µL and 9 µL for 903 card and LDC, respectively) via qPCR (**Table S3**) to determine the fold parasite enrichment, which we define as the relative amount of parasite DNA compared to host DNA, between the card and its reference, as described in Equations (1)–(5).

$$\Delta\mathrm{Ct} = \mathrm{Ct}_{\mathrm{sbp1}} - \mathrm{Ct}_{\beta-\mathrm{actin}} \quad (1)$$

$$\Delta\Delta\mathrm{Ct}_1 = \Delta\Delta\mathrm{Ct}_{\mathrm{LDC\ or\ 903\ card}} - \mathrm{Ct}_{\mathrm{Liq.\ Ref.}} \quad (2)$$

$$\mathrm{Fold\ parasite\ enrichment}_1 = 2^{-\Delta\Delta\mathrm{Ct}_1} \quad (3)$$

$$\Delta\Delta\mathrm{Ct}_2 = \Delta\Delta\mathrm{Ct}_{\mathrm{LDC}} - \mathrm{Ct}_{\mathrm{903\ card}} \quad (4)$$

$$\mathrm{Fold\ parasite\ enrichment}_2 = 2^{-\Delta\Delta\mathrm{Ct}_2} \quad (5)$$

We normalized the measured Ct of the parasite gene (*sbp1*) to the host gene (*β-actin*) using Equation (1). To compare the 903 card and LDC performance versus liquid blood, we calculated the difference in ΔCt between each card and its volume-matched, liquid reference using Equation (2). Then, we calculated the fold parasite enrichment for each card versus its matched liquid reference using Equation (3). As the 903 card is the standard for collection and dried storage of malaria-infected blood samples, we also calculated the difference in ΔCt between the LDC and

the 903 card—with the 903 card as the reference sample—using Equation (4). We obtained a second fold parasite enrichment for the LDC over the 903 card using Equation (5). A fold parasite enrichment of greater than 1 represents an increase in the amount of parasite DNA present in each sample type compared to its control, while a fold parasite enrichment of less than 1 represents a decrease in the amount of the parasite DNA. Results indicate a negligible, average fold parasite enrichment of 1.2 for the 903 card versus its liquid reference (**Figure 2A**). Promisingly, we demonstrate a substantially improved fold parasite enrichment of 243.2 and 139.6 for LDC compared to its liquid reference and the 903 card, respectively.

2.4 Analyzing parasite recovery using a clinical population

We obtained venous blood from 16 malaria-infected patients attending the Ewim polyclinic in Cape Coast, Ghana with WBC and parasite counts ranging from 3,800–20,100 WBC μL^{-1} and 33–251,100 parasites μL^{-1} (**Table S4**). At the clinic site, we applied 50 µL of venous blood from each patient via pipette to each replicate zone of a 903 card and an LDC (N = 5 zones per card type per patient, **Figure S4** and **Figure S5**). After drying in ambient conditions for 4 hours, cards were bagged in barrier pouches with silica desiccant and stored for up to 7 days at ambient conditions in the laboratory in Accra. In addition to the cards, we saved and froze a liquid blood sample from each patient. We shipped both card types together by FedEx at ambient conditions between the Accra laboratory and our laboratory at Tufts University (Medford, MA), which took 7 days. We shipped liquid blood samples on dry ice. Upon arrival, we immediately stored cards and liquid samples at -20 °C until they could be processed. We extracted DNA from both card types and matched, whole blood reference samples (50 µL and 9 µL for 903 card and LDC, respectively), and we performed qPCR to obtain *β-actin* and *sbp1* Ct values (**Table S5**). Unlike *in vitro* samples, DNA extracted from clinical samples had to be amplified across multiple PCR plates due to the evaluation of 16 patients, each with 3 sample types (903 card, LDC, and liquid blood), and with 3 technical replicates each. We used an inter-plate calibrator sample (IPC) with a known WBC and

parasite count to normalize for plate-to-plate variability. Using the IPC, we normalized the raw Ct values from each plate (N = 9 plates) using Equation (6)[29] to obtain "corrected" Ct (**Table S6**) that we used for subsequent calculations (**Table S7**).

$$\mathrm{Ct}_{\mathrm{i}}^{\mathrm{corrected}} = \mathrm{Ct}_{\mathrm{i}}^{\mathrm{uncorrected}} - \mathrm{Ct}_{\mathrm{i}}^{\mathrm{IPC}} + \frac{1}{\#\ \mathrm{of\ plates}} \sum_{\mathrm{i}=1}^{\#\ \mathrm{of\ plate}} \mathrm{Ct}_{\mathrm{i}}^{\mathrm{IPC}} \quad (6)$$

Because volumes of all samples are known precisely, we can use measured Cts to determine parasite enrichment (**Table S8**). Results again indicate negligible fold parasite enrichment of 1.2 for the 903 card versus the liquid reference (**Figure 2B**). Encouragingly, the LDC demonstrated improved enrichment of parasite DNA with average fold parasite enrichment of 32.5 and 36.6 compared to its matched liquid reference and the 903 card, respectively.

To better understand the cause of differences in fold parasite enrichment observed between *in vitro* and clinical samples for the LDC, we compared the Ct values of the *sbp1* gene (**Figure 3**). While we observed a statistically significant loss of parasites in the 903 card, as determined by linear regression comparison analysis (ANCOVA, α = 0.05, p = 0.002), we observed no significant loss in parasites for LDC (p = 0.497) (**Table S9**). To provide a better context for the clinical samples, we converted raw Ct values into WBC and parasite counts using calibration curves (**Figure S6**). We report WBC and parasite counts as total counts per extracted sample (**Table S10**). We then calculated the recovery of WBC and parasites in punches from each card using the matched liquid reference sample (**Table S11** and **Table S12**, respectively). **Table 1** illustrates the average recovery of WBCs and parasites from 903 cards and the LDC. Interestingly, we observed that both cards substantially deplete WBCs (< 18% recovered from both cards); however, the data also suggest that 903 cards deplete parasites with an average of only 18% of the parasites recovered. Since the entire 50 µL zone is extracted from the 903 card, we would not anticipate any parasite or WBC loss. This result highlights a potential problem with DNA stability

in the 903 card. In contrast, LDC showed 126.2% parasite recovery, suggesting that LDC stabilizes DNA and may enrich parasites at the extraction zone in comparison to whole blood. For the LDC, only 1 of the 16 patients (Patient 16) demonstrated poor WBC depletion, with 88.5 ± 42% WBC recovery at the extraction zone. The 15 other patients retained an average of only 12.4% of WBCs at the extraction zone. Based on visual inspection of the LDC for Patient 16 (**Figure S5**), we believe this discrepancy may be due to overloading this LDC with > 50 µL of blood as their hematocrit (31.5%) should not result in the complete saturation of the device overflow channel.

2.5 Analysis of blood drying times for each card type

While DBS cards like the 903 card can provide advantages over vacutainers for storing blood, they are not intended for long term-storage at ambient conditions, and it is recommended that 903 cards are stored at -20 °C with desiccant to minimize the possibility of sample degradation over time.[30] As both cards types were stored for 14–16 days at ambient temperatures prior to storage at -20 °C, it is possible that a combination of drying speed[31] and storage conditions[30] (e.g., temperature) led to poor DNA stability in the 903 card, while the construction of the LDC could have overcome these same conditions. A polyester-based membrane (Leukosorb) rather than a cellulosic material (Whatman 903) was used in the LDC. In addition, the LDC design provided a larger sample collection area than the 903 card (180 mm^2 versus 125 mm^2). Both factors should enable faster drying of an equal volume of collected blood for the LDC over the 903 card (ca. 2–4 hours)[32,33] Importantly, while maximizing the LDC surface area, we kept in mind a geometry that would: (i) allow for hematocrit-independent filling with a 50 µL sample and (ii) present clearly defined sample application and extraction zones. To directly test the drying time, we applied 50 µL of blood to the 903 card and LDC (N = 3 replicates per card type) and quantified loss of mass due to evaporation over time with an analytical balance. Results show LDCs dry over two times faster than 903 cards (**Figure S7**) with initial drying rates of 0.65 and 0.31 mg min^{-1}, respectively.

These differences in rates led to average drying times of 72 ± 2 minutes and 193 ± 13 minutes (Student's t-test, $p < 0.001$), respectively. In addition to drying time, the storage of these cards at ambient and likely fluctuating conditions over a period of many days during transport between laboratories may have also played a role in degrading DNA stored in the 903 card, which would present as a depletion of WBCs or parasites by qPCR. Even if shipping conditions were responsible for the reduced recovery of DNA by 903 cards, these identical conditions did not have a negative impact on the performance of the LDC.

2.6 Targeted Illumina sequencing of P. falciparum

To examine the benefit of leukodepletion in the LDC, we selected 3 of the 16 patient samples to analyze by targeted sequencing of *P. falciparum* DNA. These patients presented with a range of WBC counts (5340–7600 μL^{-1}) and parasite counts (56–46909 μL^{-1}). We performed selective whole genome amplification (sWGA)[34] to amplify *P. falciparum* DNA and then subjected all amplified samples to molecular inversion probe (MIP) assay[35,36] prior to targeted next generation sequencing. Post-sequencing, we obtained read counts and read coverage for each sample (N = 2 replicates per patient). Results demonstrate a statistically significant improvement in read count and coverage for Patient 02 and 11 (**Figure 4**, **Table S13**). For Patient 09 (56 parasites μL^{-1}), there was no significant difference in sequencing performance between the two card types. In addition, we identified that the sequencing covered all known mutations across five key antimalarial drug resistance genes in all sequenced samples. Promisingly, the sWGA results from the LDC samples with significant improvements in read count (Patient 02 and 11) show both improved coverage and smoother coverage (i.e., uniform coverage spanning the sequenced loci per sample) across loci than the sWGA results from the 903 card (**Figure S8)**. Overall, these results demonstrate the potential of LDC to outperform traditional DBS cards in improving the quality of targeted next generation sequencing of parasite genes through leukodepletion.

Conclusion

We developed a blood microsampling device that is capable of selectively depleting host leukocytes to enrich the ratio of parasite to human DNA, with the goal of supporting efforts in malaria epidemiology by enabling the generation of high-quality sequences derived from samples collected at field sites. We designed our Leukocyte Depletion Card (LDC) to fill with blood across a wide range of hematocrits and provide a clear extraction zone for reproducible DNA extraction from the dried sample in a laboratory. We ensured the volume of blood within the extraction zone was reproducible, regardless of patient hematocrit, which enabled us to directly compare the extracted sample to a matched liquid reference volume and calculate counts of WBCs and parasites stored in each zone. In both *in vitro* models of parasite-infected blood and in a panel of blood samples collected from *Plasmodium falciparum*-infected patients at a clinical field site, the LDC outperformed the 903 card in both leukocyte depletion and the stability of parasite DNA during storage and transport of materials between laboratories. Ultimately, we demonstrated that this significant fold parasite enrichment improved read counts and read coverage for the LDC over the 903 card for parasites sequenced using selective whole genome amplification and molecular inversion probes targeting *P. falciparum* drug resistance genes. This improvement in sequence quality is enabled even by the smaller volume of blood contained in the extraction zone in the LDC (9 µL) in comparison to the 903 card (50 µL), further highlighting the advantages of simultaneous leukodepletion and DNA stabilization. While we designed the LDC to operate with fingerstick volumes of blood, this first study was enabled by blood obtained from venipuncture due to the need for approximately 1 mL of blood to permit all testing. Future research efforts that leverage the performance of the LDC will require developing protocols for the direct application of fingersticks (e.g., treatment with anticoagulant) in addition to optimizing the analysis of different parasite species, co-infections, or lower parasitemias. While we demonstrate here that the LDC can enumerate parasite burden and improve parasite sequence quality in patients infected with malaria, we expect these results will lead to new applications in clinical malaria research and

global health. In light of the well-documented performance gaps of 903 cards, the LDC represents a promising advancement in DBS technology for decentralizing sample collection and testing.

3 Experimental Section

3.1 Chemical reagents and materials

We purchased Munktell TFN paper from Laboratory Sales and Services (Somerville, NJ). We purchased Leukosorb sheets from Cytiva Life Sciences (Marlborough, MA). We purchased Fellowes and Avery laminates, and 6 mm hole punch from Amazon. We purchased 1⁄4" clear acrylic sheets from McMaster-Carr. We purchased sterile pipette tips from Mettler Toledo (Columbus, OH). We purchased 40-mm microhematocrit capillary tubes from LW Scientific. We obtained samples of whole blood collected in potassium EDTA vacutainers from Research Blood Components (Watertown, MA). We purchased Drabkin's reagent, Brij 35 (30% w/w), and ASTM Type I water from Ricca Chemical (Arlington, TX). We purchased Critoseal vinyl plastic putty and 2 mL microcentrifuge tubes from VWR. We purchased QiAamp DNA Mini kits from Qiagen (Germantown, MD). We purchased Whatman 903 Protein Saver cards from Fisher Scientific (Hampton, NH). We purchased 100% ethanol, 96-well qPCR plates, MicroAmp optical adhesive film, Fast SYBR Green Master Mix, and Qubit 1X dsDNA High Sensitivity Kit from Thermo Fisher (Waltham, MA). We purchased *β-actin* forward and reverse primers, *sbp1* forward and reverse primers, and 13 primers for sWGA that were modified with phosphorothioate from Integrated DNA Technologies (Coralville, IA). We purchased RNase P from LGC SeraCare (Milford, MA). We purchased RPMI medium from KD Biomedical (Columbia, MD). We purchased $NaHCO_3$ (pH 7.3), gentamicin, and 10% human serum from Interstate Blood Bank (Memphis, TN), and 0.5% Albumax II (Gibco, Waltham, MA). We purchased Giemsa stain and sorbitol from Sigma Aldrich. We purchased MIP reagents as described previously.[36]

3.2 Live subject statement

We obtained samples of whole blood from Research Blood Components (Watertown, MA). The vendor follows the American Association of Blood Banks guidelines for all donors, which includes IRB approved consent to the use of collected blood for research purposes. All research was approved by the Institutional Biosafety Committees of Tufts University and Uniformed Services University of the Health Sciences.

3.3 Patient participation and consent (Cape Coast, Ghana)

The clinical study in Cape Coast, Ghana was approved by the Institutional Review Board of the Noguchi Memorial Institute for Medical Research (CPN# 050/12-13). Participants of all age groups were eligible to be enrolled into the study. Prior to enrollment, we obtained written informed consent from all adults with parental consent provided by the parent/guardian of all children below the age of 18 years. All samples were obtained from Ewim Polyclinic in Cape Coast, Central Region of Ghana.

3.4 Fabricating leukocyte depletion cards

We designed four dried blood spot cards in Adobe Illustrator (prototypes 1–4). We utilized a double-sided wax transfer method to pattern the TFN with unique designs on each side.[37] Briefly, we printed the top and bottom designs onto Avery laminate sheets using a Xerox ColorQube 8580 wax printer. Next, we aligned a sheet of TFN with the top and bottom designs using a custom acrylic alignment jig. Finally, we used a VEVOR P8200 T-shirt press (50 s at 142 °C) to transfer the wax from the laminate sheets to the paper to form hydrophobic barriers through the full thickness of the paper. We cut Leukosorb circles or channels using an OMTech laser engraving machine (Anaheim, CA). We fabricated each card by attaching layers with laser-cut adhesive sheets and sealed each card using Fellowes laminates.

3.5 Measuring and adjusting the hematocrit from whole blood samples

We measured the initial hematocrit of each donor whole blood sample upon arrival using centrifugation (3 µL into a capillary and spun for 3 min at 12,000 rpm in an LW Scientific ZipCombo centrifuge). We created samples of whole blood at different hematocrit values (25–55%) by adjusting the volume of native plasma in the sample using previously described methods.[22] We then confirmed the hematocrit value by centrifugation (N = 2 capillary tubes per contrived hematocrit).

3.6 In vitro P. falciparum culture conditions

We obtained *P. falciparum* strain NF54 through BEI Resources (MRA-1000, Patient Line E, contributed by Megan G. Dowler). In brief, we maintained parasites in an atmosphere of $N_2/CO_2/O_2$: 90/5/5 and complete RPMI medium (RPMI 1640, 25 mM HEPES, 100 µg mL^{-1} hypoxanthine, 0.3 mg mL^{-1} glutamine) supplemented with 25 mM $NaHCO_3$, 5 µg mL^{-1} of gentamicin, and 10% human serum or 0.5% Albumax II. We evaluated parasitemia (Infected RBCs/Total RBCs*100) through microscopy after Giemsa staining of smears (10%, 15 minutes). We used sorbitol (5 wt%, 20 min at 37 °C) to synchronize parasites cultures in the ring-stage.

3.7 Making blood samples with contrived parasitemias to add to 903 cards and LDCs

We harvested sorbitol-synchronized, ring stage parasite cultures, spiked these cultures into donor whole blood, and adjusted the hematocrit to 40%. We then used these samples to prepare samples of blood comprising parasitemias of 0%, 0.001%, 0.01%, 0.1%, 1% and 5% (**Table S14**). We applied 50 µL of each parasitemia to each replicate zone of a 903 card and a LDC (N = 5 replicates per card type) and stored an additional 100 µL of whole blood to serve as a control specimen.

3.8 Analyzing 903 cards and LDC with contrived parasitemias

We stored 903 cards and LDCs in foil bags at 4 °C until analysis. For LDCs, we used a standard 6 mm hole punch to remove the extraction zones from a LDC (N = 5 replicates, one punch per replicate zone). For 903 cards, we used a $^{5}/_{8}$" manual punch to remove the entirety of each blood spot (N = 5 replicate zones per card). We extracted genomic DNA (gDNA) from each punch (1 punch per extraction) and from liquid controls (9 or 50 µL) using a Qiagen QIAamp DNA Mini kit and according to Qiagen's dried blood spot and liquid whole blood extraction protocols. We extracted each punch separately (one punch per reaction). We used 100 µL of Qiagen QIAamp DNA Mini Kit Buffer AE (water-based elution buffer) for each final elution step and stored the purified gDNA from each sample at -20 °C until use. We amplified the *β-actin* and *sbp1* genes from each purified DNA sample using a QuantStudio3 Real Time PCR system. Briefly, each 20 µL of qPCR reaction mix contained 10 µL Fast SYBR Green Master Mix, 1.6 µL of mixed forward and reverse *β-actin* or *sbp1* primers (5 µM total per reaction, **Table S15**), 6.4 µL Type I water, and 2 µL of purified DNA. We used RNase P as the non-template control. Instrument cycling conditions are shown in **Table S16**. Example amplification and melt curves are shown in **Figure S9**. We determined fold parasite enrichment using Equations (1)–(5) (**Table S3**).

3.9 Clinical sample collection

We first identified malaria-infected patients using a blood smear. Then, we collected approximately 1 mL of blood from each consenting participant. For each sample, we spotted five 50-µL drops of blood onto unique collection zones of individually labeled Whatman 903 Protein Saver Cards and LDCs. We dried both card types at room temperature for 4 hours. Upon drying, we put both card types in individual foil bags containing a desiccant and stored each at room temperature pending analysis. The remaining blood samples were stored at -20 °C.

3.10 Determining parasite density of clinical samples using microscopy

We processed and stained blood films according to WHO guidelines.[38] We had two independent malaria microscopists read each smear, with any discordant calling of positive or negative smears broken by a third microscopist. We estimated parasite density as the number of parasites counted per 200 WBCs, multiplied by 40 based on the assumption that 1 μL of blood contains 8000 WBCs.

3.11 Analyzing 903 cards and LDCs from clinical patient samples

We handled clinical samples in an identical manner to *in vitro* samples (see Section 3.8), with a slight modification for the analysis procedure due to the number of samples we needed to process, which were analyzed across 8 PCR plates to include all 16 patients and replicates. On each plate, we included a sample (N = 3 replicates) with a single, known WBC and parasite concentration and then corrected all raw Ct values using Equation (1)[29] (**Table S5** and **Table S6** for uncorrected and corrected Ct values, respectively). Using these corrected raw Ct values, we then determined fold parasite enrichment as described using Equations (1)–(5). Calculated values are shown in **Table S7** and **Table S8**.

3.12 Analysis of card drying time

We obtained the initial mass of 903 cards and LDCs (N = 3 replicates per card type) using a Cole Palmer LA-164 balance. Then we applied 50 μL of blood to each card via pipette (at a contrived 40% hematocrit) and tracked their wet volume loss due to evaporation using RADWAG R-Lab balance tracking software until the measurements reached a plateau indicative of the residue dry volume mass. We plotted the blood spot mass as a function of time to obtain the average dry time for each card type (**Figure S7**). We approximated the average, initial rate of loss due to drying by fitting the initial linear portions of each curve.

3.13 Selective whole genome amplification

We performed selective whole genome amplification (sWGA) on extracted gDNA from three clinical patient samples, across all specimen types (903 card, LDC, and matched liquid reference samples; N = 2 replicates per patient), as described previously[34] with minor modifications. In brief, sWGA is an enrichment method to selectively amplify a target genome (here, *P. falciparum* DNA) over background DNA (here, the human genome in WBC) using a pool of primers designed to amplify frequently occurring motifs of short nucleotides in the *P. falciparum* reference genome (**Table S15**). We performed the sWGA experiment in two steps: first, we combined 8 µL of each purified gDNA sample, 0.25 µL of primers (final solution concentration of 20 µM of each primer in the pool), 0.5 µL of 10X ThermoFisher EquiPhi29 reaction buffer, and 1.25 µL of nuclease-free water. We then denatured the 10 µL reaction for 3 minutes at 95 °C. Next, we mixed the denatured product with 1 µL (10 units) of EquiPhi29 DNA polymerase, 2 µL reaction buffer, 0.2 µL of 100 µM MDT, 2 µL of 10 mM dNTPs, and nuclease-free water to make a total pool volume of 20 µL. We incubated the reaction at 45 °C for 3 hours and then at 65 °C for 10 minutes to suspend further enzyme activity. We validated amplification success by quantifying DNA before and after enrichment using a Qubit fluorometer and Qubit 1X dsDNA High Sensitivity Kit.

3.13 MIP sequencing and data analysis

We targeted, captured, and sequenced sWGA-amplified DNA using molecular inversion probes (MIP) targeting key *P. falciparum* drug resistance genes associated with artemisinin and partner drug resistance, including *pfkelch13, pfmdr1, pfcrt, pfdhfr and and pfdhps* genes. We performed MIP capture and library preparation as previously described.[35,36] In brief, we conducted sequencing using an Illumina NextSeq 550 instrument (150 bp paired-end reads). We demultiplexed the raw data generated using MIPs using MIPtools software,[39] which is a computationally suitable tool for MIP data processing and analysis. We further processed the data using MIP Wrangler software,[40] in which sequence reads sharing the same Unique Molecular

Identifiers (UMIs) were collapsed to generate a single consensus. We analyzed each dataset by mapping sequence reads to the *P. falciparum* 3D7 reference genome using Burrows-Wheeler Aligner (BWA) to generate a total number of sequenced reads per sample and sequencing coverage per samples per MIP probe used. Then we compared the count (**Figure 5A**, **Table S13**) and coverage (**Figure 5B**, **Table S13**) across different parasite densities for each sample set (903 card versus LDC) using R software, using a *p-value* of ≤ 0.05 as statistically significant. Additionally, we analyzed several known and validated resistance markers across five key antimalarial drug resistance genes, including dhfr-ts and dhps (for SP resistance), crt (CQ marker), k13 (for partial artemisinin resistance), and mdr1 (a marker for various drugs, including CQ and AL). We determined smoothness of coverage by accessing how uniformly the coverage spans the sequenced loci per sample for the 903 card (**Figure S8A**) and LDC (**Figure S8B**).

Acknowledgements

This work was supported by an award from the Henry M. Jackson Foundation for the Advancement of Military Medicine through the Global Health Engagement Research Initiative (GHERI) and a generous gift from James Kanagy. The opinions and assertations expressed herein are those of the author(s) and do not reflect the official policy or position of the Uniformed Services University of the Health Sciences, Henry M. Jackson Foundation for the Advancement of Military Medicine, Inc., or the Department of Defense.

Conflicts of Interest

The authors declare the following competing financial interest(s): CRM, AJT, and KRB are co-inventors on patent applications for technologies related to blood microsampling devices. KCW and VAS do not have a financial interest in any commercial product, service, or organization providing financial support for this research.

Figure 1. Design of the Leukocyte Depletion Card (LDC, "*prototype 4"*) and quantification of the volume contained in the sample extraction zone. **(A)** The LDC design comprises a single-layer of Leukosorb laser-cut into a channel that is reinforced within an identically-cut layer of TFN. The design is tiled five times across the card. **(B)** Image of the upper portion of the LDC depicting an area to fill out patient information (white rectangle) as well as an (i) inlet zone (indicated to user with green arrow), (ii) separation channel, (iii) extraction zone, and (iv) overflow channel. **(C)** Representative images showing LDC channels filling across a range of hematocrits from 25–55%. **(D)** Punch zone volumes for all hematocrits were determined using Drabkin's assay (N = 3 replicate punches per hematocrit). Markers represent individual measurements, the solid green line represents the average punch volume, and the dotted green lines represent the 95% CI.

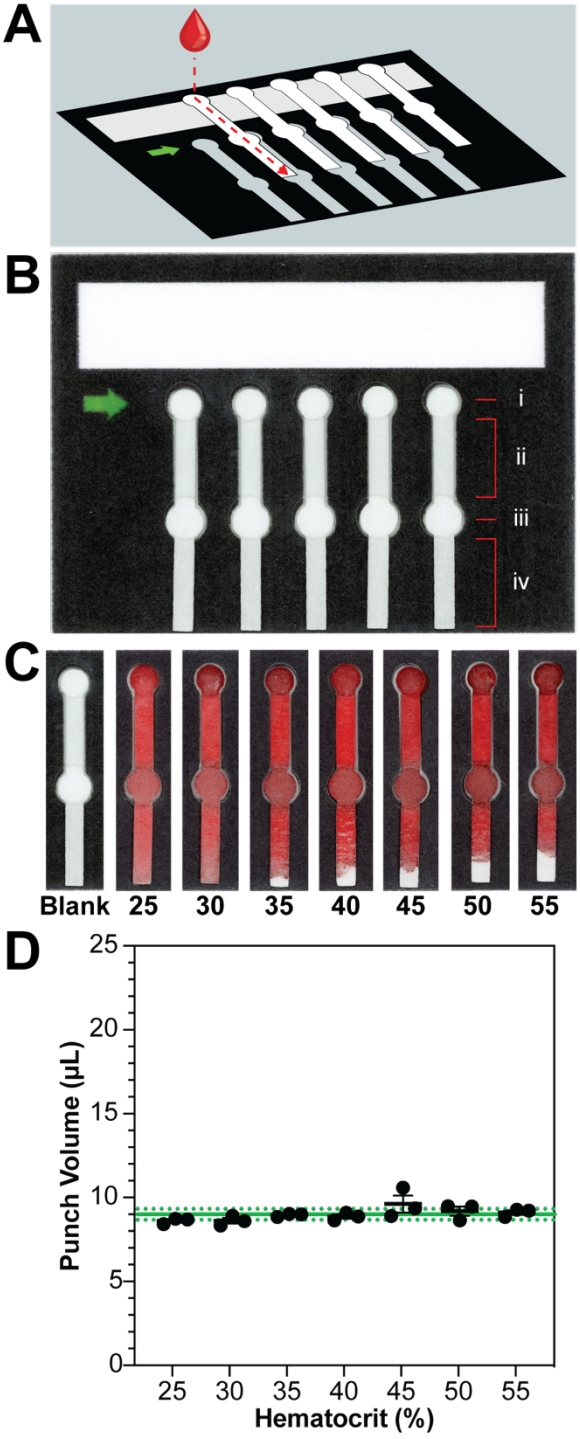

Figure 2. Fold parasite enrichment from *in vitro* and clinical samples. The Y-axis has been log-transformed for clarity. Boxes represent the 25^{th}–75^{th} percentiles, the middle line represents the median value, and whiskers represent the 5–95% percentiles. We calculated relative parasite to host enrichment by first comparing the gene of interest (*sbp1*) with the reference gene (*β-actin*) for each sample (ΔCt), then comparing the difference between these values for each card type (ΔΔCt), and finally calculating fold gene expression ($2^{-\Delta\Delta Ct}$). **(A)** Fold parasite enrichment from *in vitro* samples using blood from a single donor supplemented with cultures of parasitized RBCs. Each data set represents five parasitemias (0.001%, 0.01%, 0.1%, 1%, and 5%) with five replicates per parasitemia for a total of 25 measurements per comparison. Visualized data points represent values (2/25 points per comparison) that fall outside of the 5–95% percentiles. **(B)** Fold parasite enrichment from clinical samples collected from malaria-infected patients. Each data set represents 16 patients (N = 3 replicates per patient for a total of 48 measurements). Visualized data points represent values (4/48 points per comparison) falling outside of the 5–95% percentiles.

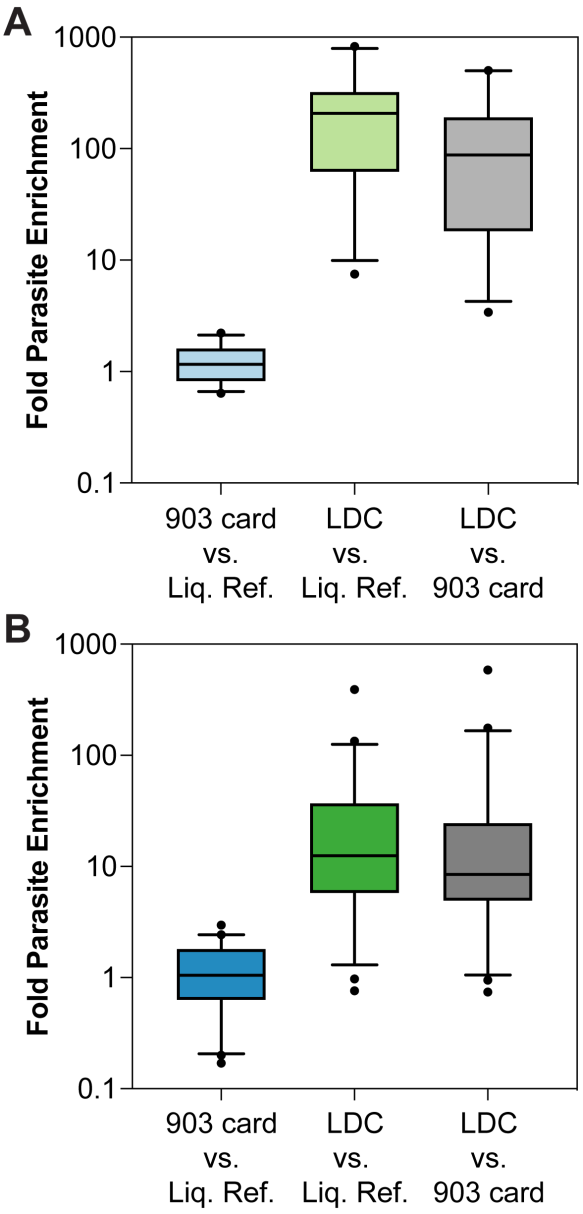

Figure 3. Comparison of *P. falciparum* gene amplification trends using *in vitro* and clinical samples of whole blood. We amplified the malaria *sbp1* gene by qPCR and plotted the measured Ct as a function of parasite count for samples collected with **(A)** 903 cards and **(B)** LDCs using *in vitro* (n = 5 contrived parasitemias, N = 5 replicates per parasitemia) and clinical samples (n = 15 unique patients, N = 3 replicates per patient). We removed the results from one patient, Patient 14, from this analysis due to an undefined *sbp1* Ct value.

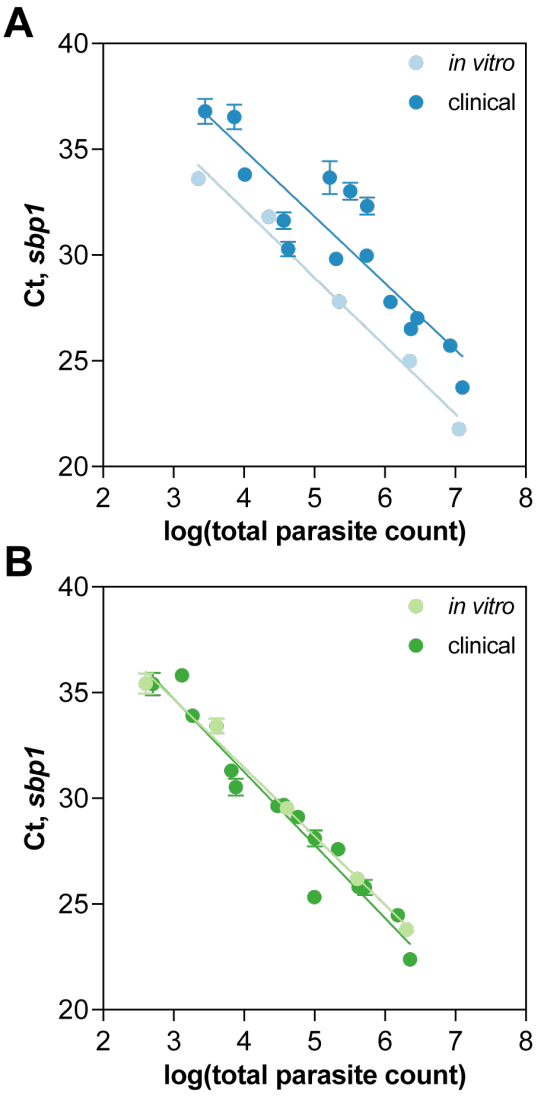

Table 1. WBC and Parasite Recovery from Clinical Blood Samples by 903 Cards and LDCs

	WBC Recovery (%)		Parasite Recovery (%)	
Card	Average	95% CI	Average	95% CI
903	11.4	[8.8–14.0]	18.3	[12.2– 25.2]
LDC	17.2	[9.1–25.3]	126.2	[109.8–142.5]

Figure 4. Using clinical samples collected by 903 DBS cards and LDCs to support next generation sequencing of *P. falciparum* genomes. **(A)** We analyzed Patients 09, 02, and 11 to cover a wide range of parasite counts (56, 4046, and 46909 parasites μL^{-1}, respectively). We plotted sample read count from Illumina sequencing as a function of parasites μL^{-1}, and performed statistical comparisons of read counts from both cards for each patient (N = 2 replicates per run). **(B)** We calculated the average target coverage by dividing the paired read count by the number of probes (185) in each sample. (ns = $p > 0.05$, ** $p < 0.01$, *** $p < 0.001$)

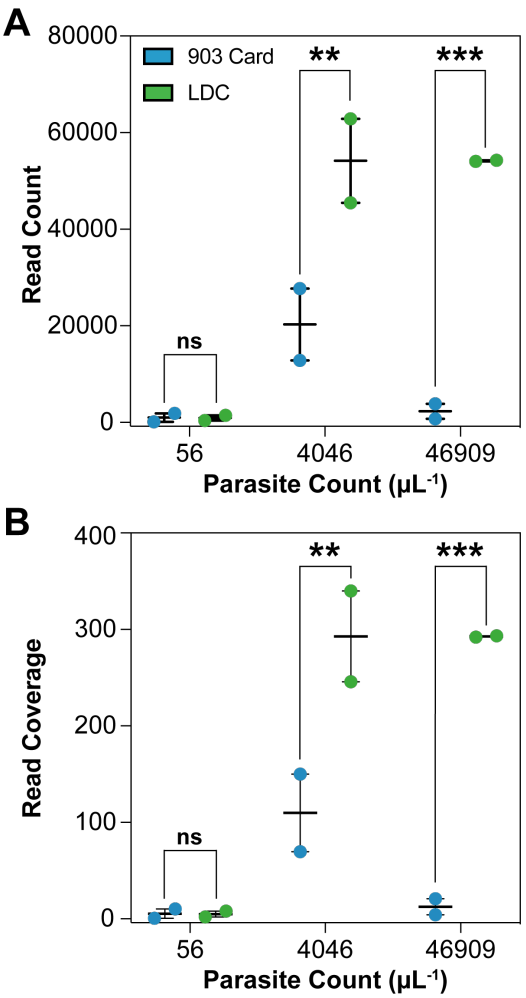

References

[1] World Health Organization, “Malaria”, can be found under https://www.who.int/news-room/fact-sheets/detail/malaria, **2023**.

[2] Kansas Department of Health and Environment, “Newborn Screening Filter Paper Dried Blood Spot Unsatisfactory Codes”, can be found under https://www.kdhe.ks.gov/DocumentCenter/View/9179/Filter-Paper-Dried-Blood-Spot-Unsatisfactory-Codes-PDF, **2021**.

[3] P. M. Edelbroek, J. van der Heijden, L. M. Stolk, *Ther. Drug Monit*. **2009**, *31*, 327.

[4] P. Denniff, N. Spooner, *Bioanalysis* **2010**, *2*, 1385.

[5] E. M. Hall, S. R. Flores, V. R. De Jesús, *Int. J. Neonatal Screen* **2015***, 1*, 69.

[6] S. O. Oyola, Y. Gu, M. Manske, T. D. Otto, J. O’Brien, D. Alcock, B. Macinnis, M. Berriman, C. I. Newbold, D. P. Kwiatkowski, H. P. Swerdlow, M. A. Quail, *J. Clin. Microbiol.* **2013**, *51*, 745.

[7] S. Auburn, S. Campino, T. G. Clark, A. A. Djimde, I. Zongo, R. Pinches, M. Manske, V. Mangano, D. Alcock, E. Anastsi, G. Maslen, B. MacInnis, K. Rockett, D. Modiano, C. I. Newbold, O. K. Doumbo, J. B. Ouédraogo, D. P. Kwiatkowski. *PLoS One* **2011**, *6*, e22213.

[8] S. O. Oyola, T. D. Otto, Y. Gu, G. Maslen, M. Manske, S. Campino,D. J. Turner, B. Macinnis, D. P. Kiatkowski, H. P. Swerdlow, M. A. Quail, *BMC Genomics* **2012** *13*.

[9] A. Melnikov, K. Galinsky, P. Rogov, T. Fennell, D. Van Tyne, C. Russ, R. Daniels, K. G. Barnes, J. Bochicchio, D. Ndiaye, P. D. Sene, D. F. Wirth, C. Nusbaum, S. K. Volkman, B. W. Birren, A. Gnirke, D. E. Neafsey. *Genome Biol.* **2011**, *12*, R73.

[10] M. Quail, T. D. Otto, Y. Gu, S. R. Harris, T. F. Skelly, J. A. McQullian, H. P. Swerdlow, S. O. Oyola, *Nat Methods* **2012**, *9*, 10.

[11] Cytiva, “Isolation of mononuclear cells”, can be found under https://cdn.cytivalifesciences.com/api/public/content/digi-16156-pdf, **2020**.

[12] H. Chen, C. M. Schürch, K. Noble, K. Kim, P. O. Krutzik, E. O'Donnell, J. Vander Tuig, G. P. Nolan, D. R. McIlwain, *BMC Immunology*, **2020**, *21*, 15.

[13] Cytiva, "Acrodisc WBC (white blood cell) syringe filter", can be found under https://www.cytivalifesciences.com/en/us/shop/lab-filtration/syringe-filters-sterile/white-blood-cell-syringe-filters/acrodisc-wbc-white-blood-cell-syringe-filter-p-36637, **2024**.

[14] D. Okuzaki, S. Kimura, N. Yabuta, T. Ohmine, H. Nojima, *BMC Clin. Pathol.* **2011**, *11*, 9.

[15] I. A. Belkacem, N. Mossadegh-Keller, P. Bourgoin, I. Arnoux, M. Loosveld, P.-E. Morange, T. Markarian, J. M. Busnel, S. Roulland, F. Galland, F. Malergue, *Adv. Sci.* **2021**, *8*, e2100323.

[16] Pall, "White blood cell isolation (Leukosorb) medium", can be found under https://shop.pall.co.uk/uk/en/medical/diagnostics/plasma-seperation/white-blood-cell-isolation-leukosorb-medium-zidgri78l4r, **2024**.

[17] K. R. Baillargeon, L. P. Murray, R. N. Deraney, C. R. Mace, *Anal. Chem.* **2020**, *92*, 16245.

[18] K. R. Baillargeon, G. G. Morbioli, J. C. Brooks, P. R. Miljanic, C. R. Mace, *ACS Meas. Sci. Au* **2022**, *2*, 457.

[19] M. M. Ippolito, K. A. Moser, J-B. B. Kabuya, C. Cunningham, J. J. Juliano, *Curr. Epidemiol. Rep.* **2021**, *8*, 46.

[20] World Health Organization, "Strategy to respond to antimalarial drug resistance in Africa", can be found under https://www.who.int/publications/i/item/9789240060265, **2022**.

[21] L. P. Murray, C. R. Mace, *Anal. Chim. Acta.* **2020**, *1140*, 236.

[22] S. B. Berry, S. C. Fernandes, A. Rajaratnam, N. S. DeChiara, C. M. Mace, Lab Chip **2016**, *16*, 3689.

[23] S. C. Fernandes, K. R. Baillargeon, C. R. Mace, *Anal. Methods* **2019**, *11*, 2057.

[24] L. P. Murray, C. R. Mace, *Anal. Chem.* **2022**, *94*, 10443.

[25] K. R. Baillargeon, J. C. Brooks, Philip R. Miljanic, C. R. Mace, *ACS Meas. Sci. Au* **2021**, *2*, 31.

[26] A. J. Tierney, K. C. Williamson, V. A. Stewart, C. R. Mace, *Anal. Chem.* **2024**, *96*, 1993.

[27] K. S. Akinosoglou, E. E. Solomou, C. A. Gogos, *Hematology* **2012**, *17*, 106.

[28] M. La'lang, T. I. Budhy, Rini Prastyawati, *Mal. J. Med. Health Sci.* **2021**, *17*, 111.

[29] YUMPU, "TATAA Interplate Calibrator User Manual – TATAA Biocenter" can be found under https://www.yumpu.com/en/document/view/38998447/tataa-interplate-calibrator-user-manual-tataa-biocenter, **2012**.

[30] Cytiva, "5 frequently asked questions about Whatman products" can be found under https://www.cytivalifesciences.com/en/us/news-center/5-faqs-about-whatman-products-10001?srsltid=AfmBOoo5U2f5RIzSN0YbJo_Es3dcV9ZPk9sToAfTxww1KC9cr2QuNGlV, **2020**.

[31] C. Jurado, *Encyclopedia of Forensic Sciences*, Elsevier, London, **2013**.

[32] EBF Inc, "Instructions For Use 903^{TM} Neonate Blood Collection Cards" can be found under https://ebf-inc.com/wp-content/uploads/2017/07/Instructions_for_Use_file.pdf, **2014**.

[33] K. Malsagova, A. Kopylov, A. Stepanov, T. Butkova, A. Izotov, A. Kaysheva, *Diagnostics (Basel)* **2020**, *10*, 248.

[34] S. O. Oyola, C. V. Ariani, W. L. Hamilton, M. Kekre, L. N. Amenga-Etego, A. Ghansah, G. G. Rutledge, S. Redmond, M. Manske, D. Jyothi, C. G. Jacob, T. D. Otto, K. Rockett, C. I. Newbold, M. Berriman, D. P. Kwiatkowski, *Malar. J.* **2016**, *15*, 597.

[35] R. Verity, O. Aydemir, N. F. Brazeau, O. J. Watson, N. J. Hathaway, M. K. Mwandagalirwa, P. W. Marsh, K. Thwai, T. Fulton, M. Denton, A. P. Morgan, J. B. Parr, P. K. Tumwebaze, M. Conrad, P. J. Rosenthal, D. S. Ishengoma, J. Ngondi, J. Gutman, M. Mulenga, D. E. Norris, W. J. Moss, B. A. Mensah, J. L. Myers-Hansen, A. Ghansah, A. K. Tshefu, A. C. Ghani, S. R. Meshnick, J. A. Bailey, J. J. Juliano, *Nat. Commun*. **2020**, *11*.

[36] A. A. Fola, S. M. Feleke, H. Mohammed, B. G. Brhane, C. M. Hennelly, S. A. Assefa, R. M. Crudal, E. Reichert, J. J. Juliano, J. Cunningham, H. Mamo, H. Solomon, G. Tasew, B. Petros, J. B. Parr, J. A. Bailey, *Nat. Microbiol.* **2023**, *8*, 1911.

[37] X. Li, X. Liu, *Microfluid. Nanofluid.* **2014**, *16*, 819.

[38] WHO, “Giemsa Staining of Malaria Blood Films, in malaria microscopy standard operating procedure - MM-SOP-07A”, **2016**.

[39] Github, “bailey-lab/MIPTools” can be found under https://github.com/bailey-lab/MIPTools, **2024**.

[40] Github, “bailey-lab/MIPWrangler” can be found under https://github.com/bailey-lab/MIPWrangler, **2020**.